International Journal of Astrobiology

cambridge.org/ija

Mapping the location of terrestrial impacts and extinctions onto the spiral arm structure of the Milky Way

Michael P Gillman[1], Hilary E Erenler[2] and Phil J Sutton[3]

[1]School of Life Sciences, University of Lincoln, Brayford Pool, Lincoln, LN6 7TS, UK; [2]University of Northampton, Faculty of Arts, Science and Technology, Avenue Campus, St George's Avenue, Northampton, NN2 6JD and [3]School of Mathematics and Physics, University of Lincoln, Brayford Pool, Lincoln, LN6 7TS, UK

Research Article

Cite this article: Gillman MP, Erenler HE, Sutton PJ (2019). Mapping the location of terrestrial impacts and extinctions onto the spiral arm structure of the Milky Way. *International Journal of Astrobiology* **18**, 323–328. https://doi.org/10.1017/S1473550418000125

Received: 12 February 2018
Revised: 4 April 2018
Accepted: 10 April 2018
First published online: 15 May 2018

Key words:
Density wave theory; extinctions; impact craters; spiral arm; star formation; superchrons

Author for correspondence:
Michael P Gillman, E-mail: m.gillman@lincoln.ac.uk

Abstract

High-density regions within the spiral arms are expected to have profound effects on passing stars. Understanding of the potential effects on the Earth and our Solar System is dependent on a robust model of arm passage dynamics. Using a novel combination of data, we derive a model of the timings of the Solar System through the spiral arms and the relationship to arm tracers such as methanol masers. This reveals that asteroid/comet impacts are significantly clustered near the spiral arms and within specific locations of an average arm structure. The end-Permian and end-Cretaceous extinctions emerge as being located within a small star-formation region in two different arms. The start of the Solar System, greater than 4.5 Ga, occurs in the same region in a third arm. The model complements geo-chemical data in determining the relative importance of extra-Solar events in the diversification and extinction of life on Earth.

Introduction

Density wave theory provides predictions of the structuring of spiral galaxies with sequences of star formation, gas/dust and different-aged stars through the arms (Pour-Imani *et al.*, 2016; Vallée, 2017*a*). Detailed studies of our own Galaxy (Choi *et al.*, 2014; Wu *et al.*, 2014; Hachisuka *et al.*, 2015) and others (Foyle *et al.*, 2010; Schinnerer *et al.*, 2017) empirically show increased rates of star formation in and around spiral arm structures. What are the consequences for our Solar System and life on Earth as we pass through the spiral arms of the Milky Way? The potential importance of spiral arm passage was noted in the late 1970s and early 1980s (Napier and Clube, 1979; Clube and Napier, 1984; Raup and Sepkoski, 1984) and receives occasional scrutiny, especially with respect to its effect on climate and glaciation (Gies and Helsel, 2005; Overholt *et al.*, 2009; Svensmark, 2012; Brink, 2015), the timings of extinctions (Leitch and Vasisht, 1998; Gillman and Erenler, 2008; Filopović *et al.*, 2013) and the role of gravitational perturbation when passing through regions of dense matter (Yabushita and Allen, 1989; Kataoka *et al.*, 2014; Nimura *et al.*, 2016). Other studies and critiques of periodicity in impact cratering, extinctions and climate have focussed on shorter periods potentially related to oscillations through the galactic midplane (Rampino and Stothers, 1984; Yabushita, 2002; Rohde and Muller, 2005; Lieberman and Melott, 2007; Shaviv *et al.*, 2014; Meier and Holm-Alwmark, 2017).

Evidence on Earth for the galactic journey of the Solar System is expected to be found in the stratigraphic record of biological, geophysical and chemical changes. This includes events believed to be associated with passage through the arms, e.g. high iridium-cobalt ratios suggested as being indicative of encounters with molecular clouds (Nimura *et al.*, 2016), superchrons as potential markers of inter-arm passage (Wendler, 2004) and increased impact cratering (Clube and Napier, 1984). The improved accuracy of event ages (high-precision records), longer and more complete sets of environmental proxy data and increasingly detailed understanding of the structure of the Milky Way (e.g. Urquhart *et al.*, 2014; Bland-Hawthorn and Gerhard, 2016; Vallée, 2016, 2017*a*, 2017*b*) collectively enhance opportunities for an interdisciplinary investigation of the potential effect of the galactic cycle on the Solar System. Clarifying the timings and mechanisms during galactic cycles is important to determine the extent to which Earth processes, at given points in time, can be viewed in isolation, or coupled to solar system (e.g. Milankovitch) processes and extra-Solar drivers. If this can be achieved, then the galactic cycle may provide a unified theory of extinction and origination of life on Earth (Barash, 2016).

The model presented here maps Earth and Solar System events onto the structure and substructure of the spiral arms of the Milky Way.

CAMBRIDGE UNIVERSITY PRESS

Methods

A four-arm structure is assumed, with arm centres modelled as logarithmic spirals with an equal pitch of 13° (median value for all arms; Tables 4 and 5 of Vallée, 2015). The galactic radius of the solar system was set at 8 kpc (Vallée, 2017*b*). The model uses Vallée's notation of ^{12}CO as the arm centre with more negative distances further from the galactic centre, corresponding to younger ages with passage through the arms (Vallée, 2016). The publications of Vallée cited here present summaries and meta-analyses of multiple studies of the structure of the Milky Way.

The distances between the four arm centre spirals and the ^{12}CO marker locations given in Table 5 of Vallée (2016) (illustrated in our Fig. 1, details in Appendix 1) were minimized by manipulating parameter a of the logarithmic spiral; radius is ae^{bt}, $b = \tan$ (pitch angle). For Sagittarius-Carina and Scutum-Crux-Centaurus arms, the spiral was fitted between the two observed values (also agreeing with the start of Sagittarius but not fitted to that). The shortest Euclidean distance was found for a resolution of t to the nearest 0.0001. The distance between arm tracer galactic coordinates and the corresponding ^{12}CO coordinates was also determined, independent of the fitted spirals.

The model assumes a constant relative motion of our Solar System to the spiral arms and therefore that the galactic orbit angle is proportional to age, which can be determined once the galactic period, defined here as the time for the solar system to pass through all arms and return to its original location, is known. The galactic period is constrained by estimates of the angular velocities of the Solar System and the spiral arms. Taking the weighted mean of 228 km s^{-1} for the Solar System (LSR, Table 1, Vallée, 2017*b*) and values between 200 and 160 km s^{-1} for the spiral pattern (Table 2, Vallée, 2017*b*) gives a range of galactic periods from 1750 to 720 Myr. This can be constrained further by considering superchrons as markers of inter-arm passage (Wendler, 2004). In particular, we assume that the superchrons end at a fixed distance (and therefore time) before the arms. The difference between the times of the last two superchrons (265 and 83.07 Ma, Wang *et al.*, 2016; Belica *et al.*, 2017) is therefore equivalent to the difference between the angles of the ^{12}CO centres of the two most recent arms (84.01°), giving a galactic period of 779.58 Myr. Note that while the galactic period is fixed, the passage time between the arms varies according to the structure in Fig. 1. The higher Solar System velocity relative to spiral arm pattern is consistent with the assumption that the Solar System is below the co-rotation radius and therefore, predicted to pass through the arms of the Milky Way (Vallée, 2017*a*). The process of velocity dispersion (Wielen, 1977), which arises due to local fluctuations in the gravitational field of the galaxy and alters the individual orbits of stars in the galaxy, is a potential source of time-dependent variation in our estimate of the galactic period. Current estimates put the local stellar velocity dispersion near the sun at 25 km s^{-1} (Rix and Bovy, 2013), which is an order of magnitude less than the circular orbital velocity. The review of Bland-Hawthorn and Gerhard (2016) notes the difficulty of reliably modelling the velocity dispersion of a stellar population. We also note that there is no obvious time-dependent shift in the locations of the events considered here with respect to the locations of the spiral arms.

Based on a circular orbit of radius 8 kpc and a known galactic period, an event of a given age has a location whose distance from the modelled ^{12}CO arm centre can be determined. The shortest Euclidean distance was again found by altering the value of t in the log spiral equation. We contrast the distance of events from the modelled arm centre with the distance between the observed

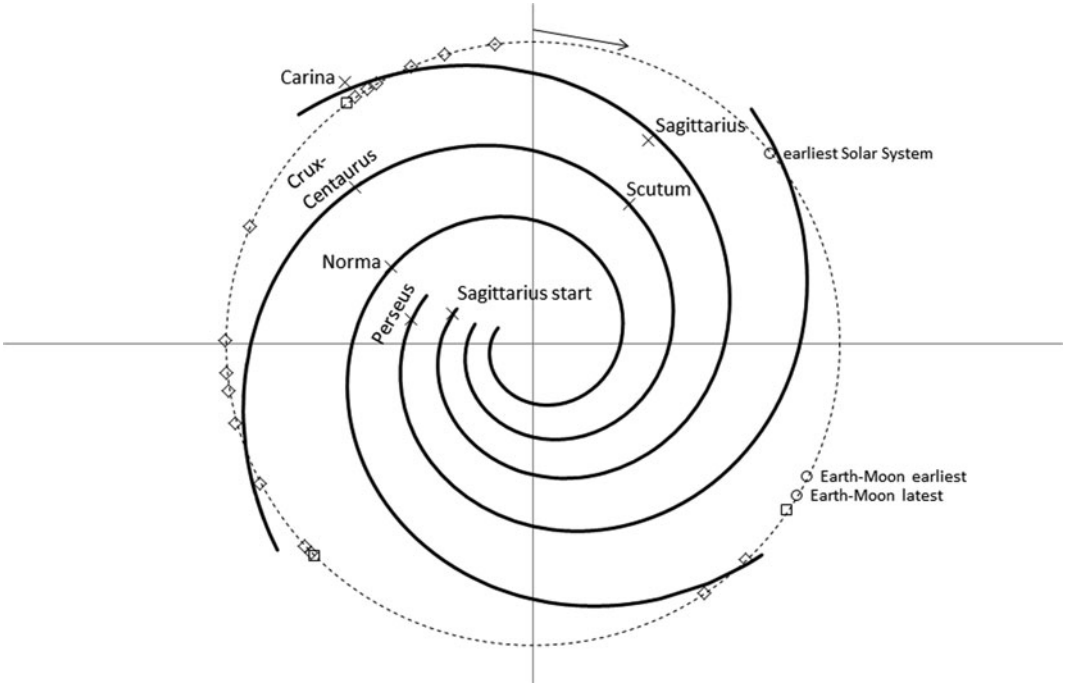

Fig. 1. Logarithmic spiral model of the Milky Way showing predicted ^{12}CO central lines and observed ^{12}CO markers (x) with arm labels. Both the spiral pattern and our Solar System (located at the top, on a radius of 8 kpc, dashed circle) move clockwise, the Solar System at a faster velocity and therefore passing through the arms. The locations of impacts (diamonds), superchron cluster midpoints (squares) and early Solar System (open circles) are shown on the Solar System orbit.

https://doi.org/10.1017/S1473550418000125 Published online by Cambridge University Press

^{12}CO location and arm tracers, including methanol masers, HI, HII, 870 μm dust and old stars (Tables 6–10 of Vallée, 2016 – our results differ from some of those presented in Table 3 of Vallée, 2016 as we use different averaged values, see Appendix 1).

The Earth and solar system events considered here (detailed in Appendix 2) comprise the largest and most accurately-aged impacts (crater diameter greater than 20 km, age error ≤4 Myr), the top three most ecologically or taxonomically severe extinctions (four extinctions in total, McGhee *et al.*, 2013), superchron ages over the last 2.2 Ga (Driscoll and Evans, 2016; Wang *et al.*, 2016; Belica *et al.*, 2017), the earliest age of the Solar System (calcium-aluminium – rich inclusions, CAIs, Connelly *et al.*, 2012; Connelly *et al.*, 2017) and the origin of the Earth-Moon system from a giant impact (Connelly and Bizzarro, 2016). The extinctions may be viewed as solely Earth-based events or an interplay of external events (e.g., impacts, molecular clouds) and Earth-based processes. Stratigraphic boundary ages and names follow Cohen *et al.* (2013) unless stated otherwise. The aim is to consider the relationship of galactic structure and arm substructure to a set of key well-dated events as a template for future work and to provide a broad base for discussion of potential mechanisms.

Three types of statistical analyses were employed. First, clustering of impacts or superchrons around the galactic orbit was tested against a Poisson distribution null model in which the probability of 0, 1, 2 … n events within an angle window are e^{-m}, me^{-m}, $(m^2/2!)e^{-m}$ … $(m^n/n!)e^{-m}$, where m is the density of events (per angle window). Superchron midpoints are assumed to be samples of the same event if they differ by less than the average duration of superchrons (details in Appendix 3). The location of clusters (mean and standard error of angle) was then compared with the independently derived locations of arm centres. Second, we determine whether Earth and Solar System events are located within one standard error of the independently derived arm tracer locations and, finally, whether the fraction of events within a given range of arm tracers is significantly different from expected (likelihood ratio test).

Times and ages are reported to the nearest 0.1 million years (abbreviated to Myr for time and Ma for age). Distances are reported to the nearest parsec. In considering these differences it should be noted that a change of 0.1° galactic longitude equates to an average of 12 pc difference, which in turn relates to about 0.8 Myr near the arm centre. Angles given in the results refer to location around the galactic centre, taking 0° as vertical and the current position of the solar system, with larger angles corresponding to earlier ages (anticlockwise in Fig. 1).

Results

The last four arm-centre (^{12}CO) interceptions are predicted to have occurred at 57.9 Ma (Carina), 239.8 Ma (Crux-Centaurus), 478.8 Ma (Norma) and 659.3 Ma (Perseus). Thirteen of the 16 impacts occur in two significant clusters around the Carina and Crux-Centaurus arms (Fig. 1), with six impacts from 6.8° to 35.2° and seven impacts from 89.5° to 134.0° ($P < 0.01$ for 29° and 45° windows respectively). The two impacts at 214.2° and 224.2° around the Norma arm have a probability of 0.07 (11° window). The means and standard errors of the first two clusters of angles (24.1° ± 4.4 and 110.4° ± 6.7) overlap with the ^{12}CO arm centre angles for Carina and Crux-Centaurus (26.7° and 110.7° respectively). The third pair of impacts with a mean of 219.2° is within 2° degrees of the Norma centre (221.1°). Five of the 11 superchron midpoints occur in two significant clusters at averages of 134.9° ($P < 10^{-4}$, 3 superchrons) and 236.4° ($P < 0.01$), 24.2° and 15.3° prior to the arm centres of Crux-Centaurus and Norma. A third cluster of two superchrons at 37.1° and 10.4° before the Carina arm is marginally non-significant ($P = 0.08$). The earliest solar system and Earth-Moon system (the midpoint of age estimates) precede the Perseus and Norma arms by 4.7° and 20.7°, respectively.

Entry into the arms occurs at about 400 pc (first marker at 440 pc, superchron end at 374 pc), with initial passage through the methanol maser and 870 μm dust regions, followed by HI after the ^{12}CO centre (Fig. 2, combining data across all four arms). The observed HII and old star regions are much wider (Fig. 2); the range of the methanol maser, HI and 870 μm dust tracers are 248 pc, 138 pc and 179 pc, respectively, compared with 828 pc and 600 pc for the HII and old star tracers (the SEs in Fig. 2 are approximately 1/6 of the full range, details of tracer locations in Appendix 1).

Thirteen of the 16 impacts occur within the widest arm regions from 440 to −660 pc (Fig. 2) equivalent to 77 Myr. The observed duration of these impacts, including errors, is from 76.5 Ma to the equivalent of 192.7 Ma (10.8 Ma), i.e. 65.7 Myr. Taking the arm tracer range as an extrinsic (and more conservative) hypothesis, the probability of 13 out of 16 events occurring in 0.395 of the time, i.e. $(4 \times 77)/779.6$, is $P = 0.0006$ ($G = 11.72$, likelihood ratio test). Two impacts prior to the earliest arm tracer in the Crux-Centaurus arm (286.2 and 1849.3 Ma) are at similar relative positions to the Earth-Moon system in the Norma arm (4426 to 4411 Ma).

The arms include the four most severe extinctions, in terms of either taxonomic ranking (end-Permian, end-Triassic and end-Ordovician) or ecological ranking (end-Permian, end-Cretaceous and end-Triassic). The end-Permian (178 pc, Crux-Centaurus) and end-Cretaceous (119 pc, Carina) extinctions are within one standard error of the methanol maser average (mean 156 ± 1 SE from 118 to 195 pc, Fig. 2). The midpoint location of the two extinctions (149 pc) is very close to the earliest solar system value (148 pc) in the Perseus arm and within 10 pc of the methanol maser average. The end-Ordovician and end-Triassic extinctions are located at −473 and −536 pc in the Norma and Crux-Centaurus arms, with separation similar to that of the end-Permian and end-Cretaceous.

Discussion

A significant fraction of the largest impacts and the top three most ecologically or taxonomically severe extinctions are located within the spiral arms according to the model presented here. A noteworthy example is the end-Cretaceous extinction, well-known as the final demise of the dinosaurs, set against a backdrop of fluctuating global climate (Bowman *et al.*, 2014; Thibault *et al.*, 2016). The proximal triggers for this extinction are debated but have centred mostly on the Chicxulub impact (Renne *et al.*, 2013) and the Deccan traps (Parisio *et al.*, 2016). Nimura *et al.* (2016) use the iridium-cobalt ratio as an extraterrestrial index to hypothesize interactions with a giant molecular cloud from about 71 to 65 Ma (using 66 Ma as the end-Cretaceous age), overlapping with intermittent cooling from about 71.6 to 66.4 Ma (Thibault *et al.*, 2016). This timing is consistent with the methanol maser mean location ± 1 SE (Fig. 2), equivalent to 71.1 to 66.0 Ma. The geological study of Nimura *et al.* (2016), combined with insights into the possible effects of molecular clouds (Yabushita and Allen, 1989; Kataoka *et al.*, 2014), complements

https://doi.org/10.1017/S1473550418000125 Published online by Cambridge University Press

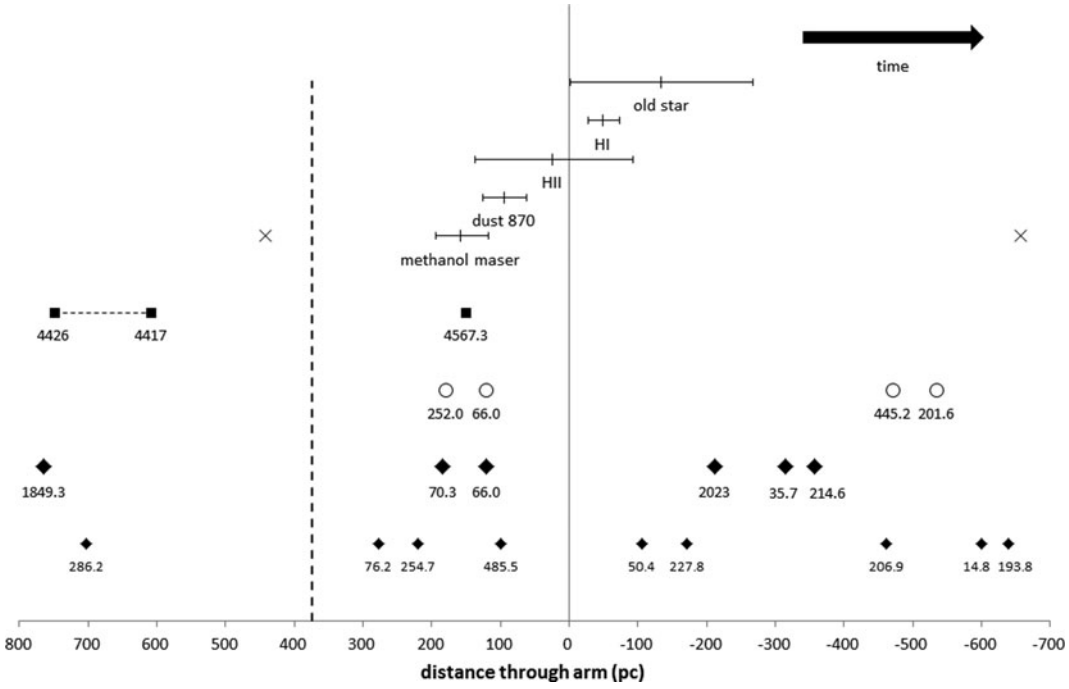

Fig. 2. Relationship of impacts (diamonds), extinctions (circles) and early solar system (squares) to arm tracer locations during passage through the spiral arms. The labels on the impacts, extinctions and solar system events are absolute ages (Ma, to nearest 0.1 million years). Ages relate to different arm passage as follows: Carina (76 to 14 Ma), Crux-Centaurus (254 to 193 Ma, 1849 Ma), Norma (485 to 445 Ma, 4420 Ma) and Perseus (4567 Ma). The impacts are divided into greater and less than 50 km diameter craters (upper and lower lines respectively, distinguished by font size). The error bars on the arm tracers are one standard error (across all arms, multiple markers within one arm are themselves averaged). The two crosses indicate the first and last arm markers. The vertical dashed line indicates the end of the last two superchrons (used in the calculation of the galactic period and assumed to be an equal distance from the arm centre). The horizontal dashed line links the age estimates for the Earth-Moon system.

the galactic model presented here. The end-Permian extinction, the most severe both taxonomically and ecologically (McGhee *et al.*, 2013), is predicted to occur in the Crux-Centaurus arm, at an approximately equal distance from the methanol maser average as the end-Cretaceous extinction.

Methanol masers are indicative of regions of high star formation (Fontani *et al.*, 2010). Indeed, the current model places the earliest age of our own Solar System (CAIs) within 10 pc of the methanol maser average in the Perseus arm. The CAIs formed from heating and rapid cooling of dust approximately 1–2 Myr after gravitational collapse within a molecular cloud (Amelin and Ireland, 2013). Passage through high mass/density regions offers various possibilities for mechanisms underpinning proximal extinction triggers, including rapid climate change (possibly due to enhanced Milankovitch effects); higher frequency of asteroid/comet impacts including extrasolar induced gravitational scattering events of minor planets (Goździewski *et al.*, 2010; Malmberg *et al.*, 2011) and orbital perturbation of Oort cloud objects (Kenyon and Bromley, 2004; Collins and Sari, 2010); increased magmatic activity (altered Earth tides) and higher cosmic ray incidence (Benyamin *et al.*, 2016). Regions of high star formation are also linked to supernovae which, along with possibly related gamma-ray bursts, have been suggested as causes of extinctions (Russell and Tucker, 1971; Ellis and Schramm, 1995; Melott *et al.*, 2004).

Evidence from our own Solar System and many recently discovered exoplanets implies gravitational scattering events are common during the dynamic evolution of planetary systems (Weidenschilling and Marzari *et al.*, 1996; Chatterjee *et al.*, 2008; Ford and Rasio, 2008; Bromley and Kenyon, 2011; Ford 2014; Batygin and Brown, 2016; Bromley and Kenyon, 2016). Furthermore, large gas giants that undergo gravitational scattering are likely to lose their moons when located >0.1 R_{Hill} from a giant gas planet (Hong *et al.*, 2018). Consequently, gravitational scattering of large planets can cause a cascade of minor planets to become de-stabilized, leading to a rise in impacts. The recent discovery of the interstellar asteroid 1I/2017 U1 in the solar system and analysis of its orbital energy suggests an extrasolar scattering (Wright, 2017).

The model presented here suggests that passage through star-formation regions may underpin the largest extinctions and that the location of the origin of our Solar System is identifiable within one such region. A dynamic model of the galactic journey of our Solar System offers the possibility to determine the extent to which that journey contributes to the stratigraphic pattern of geological change on Earth. Conversely, while the predictions of this model are clearly dependent on a set of assumptions about the dynamics and structure of the Milky Way, the increasingly accurate multi-proxy stratigraphic record may provide further checks of those assumptions. Finally, there is the opportunity to investigate the extent to which models of spiral arm passage relate to suggested shorter (quasi)periodic cycles of extinctions, impacts and climate.

Supplementary material. The supplementary material for this article can be found at https://doi.org/10.1017/S1473550418000125

Acknowledgements. We are very grateful to Jacques Vallée and Ed Gillman for advice and encouragement.

References

Amelin Y and Ireland TR (2013) Dating the oldest rocks and minerals in the Solar System. *Elements* **9**, 39–44.

Barash MS (2016) Causes of the great mass extinction of marine organisms in the Late Devonian. *Oceanology* **56**, 863–875.

Batygin K and Brown ME (2016) Evidence for a distant giant planet in the Solar System. *The Astronomical Journal* **151**(2), 22.

Belica ME *et al.* (2017) Middle Permian paleomagnetism of the Sydney Basin, Eastern Gondwana: Testing Pangea models and the timing of the end of the Kiaman Reverse superchron. *Tectonophysics* **699**, 178–198.

Benyamin D *et al.* (2016) The B/C and sub-iron/iron cosmic ray ratios – further evidence in favor of the spiral-arm diffusion model. *The Astrophysical Journal* **826**(47), 1–7.

Bland-Hawthorn J and Gerhard. O (2016) The Galaxy in context: structural, kinematic and integrated Properties. *Annual Review of Astronomy and Astrophysics* **54**, 529–596.

Bowman VC *et al.* (2014) Latest Cretaceous–earliest Paleogene vegetation and climate change at the high southern latitudes: palynological evidence from Seymour Island, Antarctic Peninsula. *Palaeogeography, Palaeoclimatology, Palaeoecology* **408**, 26–47.

Brink H-J (2015) Periodic signals of the Milky Way concealed in terrestrial sedimentary basin fills and in planetary magmatism? *International Journal of Geosciences* **6**, 831–845.

Bromley BC and Kenyon SJ (2011) A new hybrid N-body-coagulation code for the formation of gas giant planets. *The Astrophysical Journal* **731**(2), 101.

Bromley BC and Kenyon SJ (2016) Making planet nine: a scattered giant in the outer Solar System. *The Astrophysical Journal* **826**(1), 64.

Chatterjee S *et al.* (2008) Dynamical outcomes of planet-planet scattering. *The Astrophysical Journal* **686**(1), 580–602.

Choi YK *et al.* (2014) Trigonometric parallaxes of star forming regions in the Perseus spiral arm. *The Astrophysical Journal* **790**(2), 99.

Clube SVM and Napier WM (1984) Comet capture from molecular clouds: a dynamical constraint on star and planet formation. *Monthly Notices Royal Astronomical Society* **208**, 575–588.

Cohen KM *et al.* (2013) (v 2017-02), The ICS International Chronostratigraphic Chart. *Episodes* **36**, 199–204.

Collins BF and Sari R (2010) A unified theory for the effects of stellar perturbations and galactic tides on Oort cloud comets. *The Astronomical Journal* **140**(5), 1306–1312.

Connelly JN and Bizzarro M (2016) Lead isotope evidence for a young formation age of the Earth–Moon system. *Earth and Planetary Science Letters* **452**, 36–43.

Connelly JN *et al.* (2012) The absolute chronology and thermal processing of solids in the solar protoplanetary disk. *Science* **338**, 651–655.

Connelly JN, Bollard J and Bizzarro M (2017) Pb-Pb chronometry and the early Solar System. *Geochimica et Cosmochimica Acta* **201**, 345–363.

Driscoll PE and Evans DAD (2016) Frequency of Proterozoic geomagnetic superchrons. *Earth and Planetary Science Letters* **437**, 9–14.

Ellis J and Schramm DN (1995) Could a nearby supernova explosion have caused a mass extinction? *PNAS* **92**, 235–238.

Filopović MD *et al.* (2013) Mass extinction and the structure of the Milky Way. *Serbian Astronomical Journal* **1**, 1–6.

Fontani F, Cesaroni R and Furuya RS (2010) Class I and Class II methanol masers in high-mass star forming regions. *Astronomy and Astrophysics* **517**, A56.

Ford EB (2014) Architectures of planetary systems and implications for their formation. *PNAS* **111**(35), 12616–12621.

Ford EB and Rasio FA (2008) Origins of eccentric extrasolar planets: testing the planet-planet scattering model. *The Astrophysical Journal* **686**(1), 621–636.

Foyle K *et al.* (2010) Arm and interarm star formation in spiral galaxies. *The Astrophysical Journal* **725**(1), 534–541.

Gies DR and Helsel JW (2005) Ice Age Epochs and the Sun's path through the Galaxy. *The Astrophysical Journal* **626**, 844–848.

Gillman MP and Erenler HE (2008) The galactic cycle of extinction. *International Journal of Astrobiology* **7**, 17–26.

Goździewski K *et al.* (2010) Making extrasolar planets from solar systems via dynamical interactions. *European Astronomical Society Publications Series* **42**, 375–383.

Hachisuka K *et al.* (2015) Parallaxes of star-forming regions in the outer spiral arm of the Milky Way. *The Astrophysical Journal* **800**(1), 2.

Hong YC *et al.* (2018) Innocent bystanders: orbital dynamics of exomoons during planet-planet scattering. *The Astrophysical Journal* **852**(2), 85.

Kataoka R *et al.* (2014) The Nebula Winter: The united view of the snowball Earth, mass extinctions, and explosive evolution in the late Neoproterozoic and Cambrian periods. *Gondwana Research* **25**, 1153–1163.

Kenyon SJ and Bromley BC (2004) Stellar encounters as the origin of distant Solar System objects in highly eccentric orbits. *Nature* **432**, 598–602.

Leitch EM and Vasisht G (1998) Mass extinctions and the Sun's encounters with spiral arms. *New Astronomy* **3**, 51–56.

Lieberman BS and Melott AL (2007) Considering the case for biodiversity cycles: re-examining the evidence for periodicity in the fossil record. *PloS ONE* **2**(8), e759:1–9.

Malmberg D, Davies MB and Heggie DC (2011) The effects of fly-bys on planetary systems. *Monthly Notices Royal Astronomical Society* **411**(2), 859–877.

McGhee GR *et al.* (2013) A new ecological-severity ranking of major Phanerozoic biodiversity crises. *Palaeogeography, Palaeoclimatology, Palaeoecology* **370**, 260–270.

Meier MMM and Holm-Alwmark S (2017) A tale of clusters: No resolvable periodicity in the terrestrial impact cratering record. *Monthly Notices Royal Astronomical Society* **467**, 2545–2551.

Melott AL *et al.* (2004) Did a gamma-ray burst initiate the late Ordovician mass extinction? *International Journal of Astrobiology* **3**, 55–61.

Napier WM and Clube SVM (1979) A theory of terrestrial catastrophism. *Nature* **282**, 455–459.

Nimura T, Ebisuzaki T and Maruyama S (2016) End-Cretaceous cooling and mass extinction driven by a dark cloud encounter. *Gondwana Research* **37**, 301–307.

Overholt AC, Melott AL and Pohl M (2009) Testing the link between terrestrial climate change and galactic spiral arm transit. *The Astrophysical Journal* **705**, L101–L103.

Parisio L *et al.* (2016) $^{40}Ar/^{39}Ar$ ages of alkaline and tholeiitic rocks from the northern Deccan Traps: implications for magmatic processes and the K–Pg boundary. *Journal of the Geological Society* **173**, 679–688.

Pour-Imani H *et al.* (2016) Strong evidence for the density-wave theory of spiral structure in disk galaxies. *The Astrophysical Journal Letters* **827**, L2.

Rampino MR and Stothers RB (1984) Terrestrial mass extinctions, cometary impacts and the Sun's motion perpendicular to the galactic plane. *Nature* **308,** 709–712.

Raup DM and Sepkoski JJ (1984) Periodicity of extinctions in the geologic past. *PNAS* **81**, 801–805.

Renne PR *et al.* (2013) Time scales of critical events around the Cretaceous-Paleogene boundary. *Science* **339**, 684–687.

Rix HW and Bovy J (2013) The Milky Way's stellar disk. *The Astronomy and Astrophysics Review* **21**(1), 61.

Rohde RA and Muller RA (2005) Cycles in fossil diversity. *Nature* **434**, 208–210.

Russell D and Tucker W (1971) Supernovae and the extinction of the Dinosaurs. *Nature* **229**, 553–554.

Schinnerer E *et al.* (2017) The PdBI Arcsecond Whirlpool Survey (PAWS): the role of spiral arms in cloud and star formation. *The Astrophysical Journal* **836**(1), 62.

Shaviv NJ, Prokoph A and Veizer J (2014) Is the Solar System's galactic motion imprinted in the Phanerozoic climate? *Scientific Reports* **4**, 6150.

Svensmark H (2012) Evidence of nearby supernovae affecting life on Earth. *Monthly Notices Royal Astronomical Society* **423**, 1234–1253.

Thibault N *et al.* (2016) Late Cretaceous (late Campanian–Maastrichtian) sea-surface temperature record of the Boreal Chalk Sea. *Climate of the Past* **12**, 429–438.

Urquhart JS *et al.* (2014) The RMS survey: galactic distribution of massive star formation. *Monthly Notices Royal Astronomical Society* **437**, 1791–1807.

Vallée JP (2015) Different studies of the global pitch angle of the Milky Way's spiral arms. *Monthly Notices Royal Astronomical Society* **450**, 4277–4284.

Vallée JP (2016) A substructure inside spiral arms, and a mirror image across the Galactic Meridian. *The Astrophysical Journal* **821**, 53.

https://doi.org/10.1017/S1473550418000125 Published online by Cambridge University Press

Vallée JP (2017a) A guided map to the spiral arms in the galactic disk of the Milky Way. *Astronomical Review* **13**, 113–146.

Vallée JP (2017b) Recent advances in the determination of some Galactic constants in the Milky Way. *Astrophysics and Space Science* **362**, 79.

Wang T *et al.* (2016) High-precision U–Pb geochronologic constraints on the Late Cretaceous terrestrial cyclostratigraphy and geomagnetic polarity from the Songliao Basin, Northeast China. *Earth and Planetary Science Letters* **446**, 37–44.

Wendler J (2004) External forcing of the geomagnetic field? Implications for the cosmic ray flux-climate variability. *Journal of Atmospheric and Solar-Terrestrial Physics* **66**, 1195–1203.

Weidenschilling SJ and Marzari F (1996) Gravitational scattering as a possible origin for giant planets at small stellar distances. *Nature* **384**, 619–621.

Wright JT (2017) On distinguishing interstellar objects Like 'Oumuamua from products of solar system scattering. *Research Notes American Astronomical Society* **1**(1), 38.

Wielen R (1977) The diffusion of stellar orbits derived from the observed age-dependence of the velocity dispersion. *Astronomy and Astrophysics* **60**, 263–275.

Wu YW *et al.* (2014) Trigonometric parallaxes of star-forming regions in the Sagittarius spiral arm. *Astronomy & Astrophysics* **566**, A17.

Yabushita S and Allen AJ (1989) On the effect of accreted interstellar matter on the terrestrial environment. *Monthly Notices Royal Astronomical Society* **238**, 1465–1478.

Yabushita S (2002) On the periodicity hypothesis of the ages of large impact craters. *Monthly Notices Royal Astronomical Society* **334**, 369–373.

https://doi.org/10.1017/S1473550418000125 Published online by Cambridge University Press